Hydrology and Earth System Sciences Discussions

Hydrological response unit-based blowing snow modelling over an alpine ridge

M. K. MacDonald[1], J. W. Pomeroy[1], and A. Pietroniro[2]

[1]Centre for Hydrology, University of Saskatchewan, 117 Science Place, Saskatoon, SK, S7N 5C8, Canada
[2]Water Science and Technology Directorate, Environment Canada, 11 Innovation Boulevard, Saskatoon, SK, S7N 3H5, Canada

Correspondence to: J. W. Pomeroy (john.pomeroy@usask.ca)

HESSD

7, 1167–1208, 2010

Hydrological response unit-based blowing snow modelling

M. K. MacDonald et al.

Title Page

Abstract	Introduction
Conclusions	References
Tables	Figures

Back | Close

Full Screen / Esc

Printer-friendly Version

Interactive Discussion

Abstract

Snow redistribution by wind and the resulting accumulation regimes were simulated for two winters over an alpine ridge transect located in the Canada Rocky Mountains. Simulations were performed using physically based blowing snow and snowmelt models. A hydrological response unit (HRU)-based spatial discretization was used rather than a more computationally expensive fully-distributed one. The HRUs were set up to follow an aerodynamic sequence, whereby eroded snow was transported from windswept, upwind HRUs to drift accumulating, downwind HRUs. HRUs were selected by examining snow accumulation patterns from manual snow depth measurements. Simulations were performed using two sets of wind speed forcing: (1) station observed wind speed, and (2) modelled wind speed from a widely applied empirical, terrain-based windflow model. Best results were obtained when using the site meteorological station wind speed data. The windflow model performed poorly when comparing the magnitude of modelled and observed wind speeds, though over-winter snow accumulation results obtained when using the modelled wind speeds were reasonable. However, there was a notable discrepancy (17%) between blowing snow sublimation quantities estimated when using the modelled and observed wind speeds. As a result, the end-of-winter snow accumulation was considerably underestimated (32%) when using the modelled wind speeds. That snow redistribution by wind can be adequately simulated in computationally efficient HRUs over this alpine ridge has important implications for representing snow transport in large-scale hydrology models and land surface schemes. Snow redistribution by wind was shown to significantly impact snow accumulation regimes in mountainous environments as snow accumulation was reduced to less than one-third of snowfall on windswept landscapes and nearly doubled in certain lee slope and treeline areas. Blowing snow sublimation losses were shown to be significant (approximately one-quarter of snowfall or greater).

1 Introduction

Snowpack depth and density in the alpine zone of high mountains exert a strong control on the magnitude, timing and duration of snowmelt as well as directly influencing alpine ecology and avalanche formation (Jones et al., 2001). Snowcover increases the surface albedo and cools the surface compared to snow-free zones and so there are marked differences in energy and moisture fluxes over snow-covered and snow-free surfaces, which have implications for evapotranspiration, permafrost, and glaciers. Snowpack and snowcover characteristics in alpine zones are strongly influenced by wind through the action of wind in entraining, transporting and sublimating snow (Pomeroy, 1991).

Wind transport of snow is a common phenomenon across high altitude and latitude cold regions that can significantly affect snowcover distribution patterns both during accumulation- and ablation-dominated periods. Snow transport involves the horizontal redistribution of snow. Surface snow is eroded and transported via saltation (Schmidt, 1986; Pomeroy and Gray, 1990) and suspension (Budd et al., 1966; Pomeroy and Male, 1992) from flat surfaces, hilltops, windward slopes and sparsely vegetated surfaces to topographic depressions, leeward slopes and more densely vegetated surfaces (Pomeroy et al., 1993; Liston and Sturm, 1998). The occurrence of blowing snow is dependent upon the local boundary layer meteorology and physical characteristics of the snow surface. Blowing snow can proceed when the surface wind speed exceeds a threshold wind speed dictated by the snow cohesive bond forces, which depend on the thermal and settling histories of the snowpack (Li and Pomeroy, 1997a). Snow particles transported by wind are well ventilated and undergo sublimation in the presence of an unsaturated atmosphere (Dyunin, 1959; Schmidt, 1972, 1986). Sublimation of blowing snow particles is very rapid relative to that of stationary snow on the ground. Blowing snow sublimation losses of 15 to 41% of annual snowfall have been estimated for the Canadian Prairies (Pomeroy and Gray, 1995), 28% of annual snowfall over western Canadian Arctic tundra (Pomeroy et al., 1997), 18–25% of winter precipitation over

the Alaskan arctic (Liston and Sturm, 2002) and up to 20% of the annual precipitation over certain areas of the Antarctic ice sheet (Bintanja, 1998). Since snowmelt has an extremely important role in regulating annual runoff, these sublimation losses have an important effect on the hydrology of these cold regions.

5   Estimating windflow over mountainous terrain is extremely difficult because of complex turbulence structures and divergent and convergent flow directions. This is compounded by the sparse spatial distribution of alpine wind measurements to drive any flow calculation scheme. Distributed windflow simulations over complex terrain have been made using both physically based atmospheric models, and empirical models
10   using reference station measurements of wind direction and speed. Physically based atmospheric models can be very computationally expensive compared to the hydrological models to which they may be coupled (Utnes and Eidsvik, 1996). Empirical windflow models based on terrain and vegetation parameters are much more computationally efficient than the physically based atmospheric models, can be developed
15   for a wide range of scales, and have been successful for hydrological modelling purposes. Ryan (1977) developed a windflow model for complex terrain that accounts for the sheltering and diverting effects of topography. Ryan's parameterization was incorporated in Liston and Elder's (2006) meteorological distribution system MicroMet. MicroMet generates distributed wind fields from reference wind speed and direction
20   using digital elevation (DEM) model information. Winstral et al. (2009) developed an empirical method to distribute wind fields from reference wind speed and direction from a DEM-based upwind slope parameterization and vegetation information.

    Hydrological and atmospheric models require some description of blowing snow redistribution and sublimation that is suitable for complex terrain for application to cold
25   regions (Dornes et al., 2008). The large scale of application of these models in mountain and polar environments precludes a finely distributed approach such as employed for small basins (e.g. Liston and Sturm, 1998; Essery et al., 1999). Some form of landscape aggregation is necessary and has been successfully demonstrated for mountain topography in northern Canada (MacDonald et al., 2009). MacDonald et al. built upon

Dornes et al.'s (2008) work and identified hydrological response units (HRUs) suitable for calculating snow redistribution calculations in sub-arctic mountains with moderate topographic roughness and ran a blowing snow model to estimate snow accumulation quantities that compared well to field measurements.

⁵   The objectives of this study are to identify HRUs that are suitable for simulating snow accumulation and redistribution over alpine topography in mountains with severe topographic roughness and strong winds, to assess the usefulness of a commonly applied empirical windflow estimation scheme for driving blowing snow calculations in such an environment, and to use the derived wind fields and a physically based ¹⁰ blowing snow model to estimate seasonal blowing snow transport, sublimation and redistribution fluxes at an alpine site in the Canadian Rockies. The test area is the Front Ranges of the Canadian Rocky Mountains which is characterized by extremely sharp topographic gradients and steep slopes, strong Chinook winds and other strong wind features.

¹⁵ ## 2   Study site

2.1   Site description

Fisera Ridge (hereafter FR; 50°57′ N; 115°12′ W) is an alpine ridge located within the Marmot Creek Research basin (MCRB). FR is located just above treeline, where subalpine fir and larch give away to sparse shrubs, exposed soils and grass. The ²⁰ highest elevation of FR has a western boundary with an elevation of approximately 2617 m a.s.l., and decreases in elevation in an eastern and north-eastern direction with an elevation of approximately 2317 m a.s.l. at the treeline. The predominant windflow is generally normal to FR and is northerly. The north-facing slope and the ridge-top are generally windswept and the southeast-facing slope and further downwind forested ²⁵ area are snow deposition zones. MCRB is a 9.4 km^2 watershed located in the Rocky Mountain Front Ranges in Alberta, Canada. The general aspect of MCRB is easterly.

Title Page

Abstract | Introduction

Conclusions | References

Tables | Figures

◄ | ►

◄ | ►

Back | Close

Full Screen / Esc

Printer-friendly Version

Interactive Discussion

The basin is primarily montane with subalpine forest and alpine tundra ridgetops. The basin landcover consists of dense lodgepole pine, mature spruce and subalpine fir forest at lower elevations, larch, shrubs and grasses at and just below the treeline, and talus and bare rocks in the high alpine. MCRB is underlain by glacial and post-glacial deposits ranging from 10 to 30 m depth above bedrock, except at high elevations and along portions of the creek channels (Stevenson, 1967). Seasonally frozen soils are present at higher elevations. Annual precipitation is typically around 900 mm with 60–75% being snow. Climate normals as recorded at the Kananaskis Pocaterra station (ID 3053604; 1610 m a.s.l.) range from a low of −11.1 °C in January to a high of 11.4 °C in August. Temperatures are typically colder at MCRB since it is at a higher elevation. Marmot Creek itself is a tributary of the Kananaskis River and is part of the Bow River system.

2.2 Field observations

Observations from September through April 2007/2008 and 2008/2009 were used. Meteorological observations from three stations located at FR (ridge-top, north-facing, southeast-facing), from a mid-elevation forest clearing station (UC: upper clearing) at 1845 m a.s.l. 2 km away and from a meadow station (HM: hay meadow) 4.8 km away at 1437 m a.s.l. were used (Fig. 1). The ridge-top station is located at the top of FR and measures air temperature, relative humidity, incoming shortwave radiation, incoming longwave radiation, wind speed and direction. The north-facing and southeast-facing stations are located on the northern and southern faces of FR, respectively, and measure wind speed and direction. A Geonor T200B accumulating precipitation gauge was installed in a sheltered area near the ridge-top FR station during the fall of 2008. Thus, for 2008/2009, precipitation data from the FR Geonor gauge was used. 2008/2009 FR precipitation data was correlated with precipitation data from the UC Geonor T200B accumulating precipitation gauge to develop a multiplier (1.18) to extrapolate 2006/2007 and 2007/2008 UC precipitation data to the FR site. The Geonor precipitation gauge data were corrected for undercatch according to the equation presented by MacDonald

and Pomeroy (2007). There are elevation-induced differences in precipitation between the FR and UC sites.

Manual snow surveys were performed over FR during 2007/2008 and 2008/2009. The snow survey transect extended 200 m from the NF station over FR, beyond the SF station and into the forested area (Fig. 2). This snow survey followed the modelled transect. Snow depth was measured every 1–3 m and snow density was measured every fifth depth measurement using an ESC30 snow tube when possible. The snowpack was often too shallow to measure on the windswept north-facing slope and too deep (>120 cm) to measure on the south-facing slope with the ESC30 tube. Snow pits were dug when possible at the locations shown on Fig. 2. Snow density was measured in the snow pit to depth by weighing samples obtained using a fixed triangular cutting device (Perla "Swedish Sampler"). To calculate mean SWE for an HRU, the mean measured snow density for a particular HRU was applied to each depth measurement in that HRU.

A vegetation survey was conducted along the FR snow survey on 3 July 2008. A shrub count was performed within two 9 m×9 m grids (on on the north-facing slope and one on the south-facing slope). Eight shrubs were within the north-facing slope grid and 47 shrubs were counted within the southeast-facing slope grid, yielding 0.1 shrubs·m^{-2} and 0.6 shrubs·m^{-2} on the on the north-facing and southeast-facing slopes, respectively. Twenty-three shrub height and width measurements were taken along the snow survey. Average shrub height and width along the transect were 63 cm and 108 cm, respectively. Average shrub height was 51 cm and 82 cm on the north-facing and southeast-facing slopes, respectively. Average shrub width was 107 cm and 111 cm on the north-facing and southeast-facing slopes, respectively. The shrub width measurements included the aggregation of several clumps of shrubs. Photographs taken with a camera equipped with a hemispherical lens were analyzed with GLA software (Frazer et al., 1999) to determine the leaf area index (LAI) for the spruce forest downslope from the southeast-facing station. An average LAI was 0.91 was determined.

An airborne light detection and ranging (LiDAR) data collection campaign was deployed over MCB research during August 2007. High-resolution digital elevation data was obtained. A 10 m DEM of MCB was created using this high-resolution LiDAR data using Golden Software Surfer 8.00.

3   Models used

A suite of physically based algorithms were used to simulate snow accumulation over FR. The algorithms were combined within the Cold Regional Hydrological Modelling platform (CRHM; Pomeroy et al., 2007). CRHM is an object-oriented hydrological modelling platform developed for Canadian environments (e.g. boreal forest, mountain forests, alpine tundra, muskeg, arctic tundra and prairies). The spatial discretization is in the form of HRUs as a conceptual landscape sequence or water flow cascade. CRHM has a modular structure in that the modeller creates a model by selecting from a library of process modules. The following CRHM modules were used in this study: Global and Slope_Qsi (radiation calculations with adjustments for aspect, elevation and slope), PBSM (snow transport and sublimation), EBSM (snowmelt), Needleleaf (adjusts shortwave and longwave radiation exchanges beneath needleleaf forest canopies) and Trees (accounts for canopy effects on water mass balance at the ground surface).

The snow mass balance over a uniform element of a landscape (Fig. 3) is the result of snowfall accumulation, the distribution and divergence of blowing snow fluxes both within and surrounding the element, and sublimation and melt from the snowpack. The terms presented on Fig. 3 are described in the CRHM module subsections.

3.1   Global and Slope_Qsi

The CRHM Global module calculates theoretical clear-sky direct and diffuse solar radiation. Global estimates the actual number of daily sunshine hours which is used

in EBSM. Global calculates the theoretical direct beam component of solar radiation, Q_{dir}, according to Garnier and Ohmura (1970) and the diffuse clear-sky radiation component, Q_{dif}, according to List (1968) as

$$Q_{dir} = I \cdot p^m [(\sin\theta\cos H)(-\cos A\sin Z) - \sin H(\sin A\cos Z)$$
$$+ (\cos\theta\cos H)\cos Z]\cos\delta + [\cos\theta(\cos A\sin Z) + (\sin\theta\cos Z)]\sin\delta \quad (1)$$

$$Q_{dif} = 0.5((1 - aw - ac)Q_{ext} - Q_{dir}) \quad (2)$$

where I is the intensity of extraterrestrial radiation, p is the mean zenith path transmissivity of the atmosphere, m is the optical air mass (calculated from Kasten and Young, 1989), δ is declination of the sun, θ is the latitude, H is the hour angle measured from solar noon positively towards west, A is the slope azimuth measured from the north through east, Z is the slope angle, aw is the radiation absorbed by water vapour (7%), ac is the radiation absorbed by ozone (2%) and Q_{ext} is extraterrestrial radiation on a horizontal surface at the outer limit of the earth's atmosphere.

The Slope_Qsi module calculates incident solar radiation on slopes based on the ratio of measured incident shortwave radiation on a level and the calculated clear sky direct an diffuse shortwave radiation on a level plane (from Global).

3.2 Prairie Blowing Snow Model

PBSM calculates two-dimensional blowing snow transport and sublimation rates for steady-state conditions over a landscape element using mass and energy balances. PBSM was initially developed for application over the Canadian Prairies, characterized by relatively flat terrain and homogeneous crop cover (e.g. Pomeroy, 1989; Pomeroy et al., 1993). Versions have been applied to variable vegetation height (Pomeroy et al., 1991), over alpine tundra (Pomeroy, 1991), arctic tundra (Pomeroy and Li, 2000) and mountainous subarctic terrain (MacDonald et al., 2009). Only key equations are presented here. Refer to Pomeroy and Gray (1990), Pomeroy and Male (1992), Pomeroy et al. (1993) and Pomeroy and Li (2000) for further details.

Hydrological response unit-based blowing snow modelling

M. K. MacDonald et al.

Full Screen / Esc

Printer-friendly Version

Interactive Discussion

The snow mass balance over a uniform element of a landscape (e.g. a HRU) is a result of snowfall accumulation and the distribution and divergence of blowing snow fluxes both within and surrounding the element given by

$$\frac{dS}{dt}(x) = P - p\left[\nabla F(x) + \frac{\int E_B(x)dx}{x}\right] - E - M \tag{3}$$

where dS/dt is the surface snow accumulation (kg m^{-2} s^{-1}), P is snowfall (kg m^{-2} s^{-1}), p is the probability of blowing snow occurrence within the landscape element, F is the blowing snow transport out of the element (kg m^{-2} s^{-1}) which is the sum of snow transport in the saltation and suspension layers, F_{salt} and F_{susp}, $\int E_B(x)dx$ is the vertically integrated blowing snow sublimation rate (kg m^{-1} s^{-1}) over fetch distance x (m), E is the snowpack sublimation (kg m^{-2} s^{-1}) and M is snowmelt (kg m^{-2} s^{-1}).

Since PBSM is for fully-developed blowing snow conditions, PBSM is restricted to minimum fetch distances of 300 m following measurements by Takeuchi (1980). Blowing snow transport fluxes are the sum of snow transport in the saltation and suspension layers, F_{salt} and F_{susp} (kg m^{-1} s^{-1}), respectively. Saltation of snow must be initiated before snow transport can occur in the suspension layer and blowing snow sublimation can occur.

F_{salt} is calculated by partitioning the atmospheric shear stress into that required to free particles from the snow surface, to that applied to nonerodible roughness elements and to that applied to transport snow particles (Pomeroy and Gray, 1990) as

$$F_{salt} = \frac{c_1 e \rho u_{*t}}{g}\left(u_*^2 - u_{*n}^2 - u_{*t}^2\right) \tag{4}$$

where c_1 is the dimensionless ratio of saltation velocity to friction velocity ($up/u^*=2.8$), e is the dimensionless efficiency of saltation ($1/4.2u_*$), ρ is atmospheric density (kg m^{-3}), g is acceleration due to gravity (m s^{-2}), u_* is the atmospheric friction velocity (m s^{-1}), and u_{*n} and u_{*t} refer to the portions of the u_* applied to nonerodible roughness elements such as vegetation (nonerodible friction velocity) and the open snow surface

Title Page

Abstract | Introduction

Conclusions | References

Tables | Figures

◄ | ►

◄ | ►

Back | Close

Full Screen / Esc

Printer-friendly Version

Interactive Discussion

itself (threshold friction velocity), respectively. Mechanical turbulence controls atmospheric exchange during blowing snow, thus u_* is calculated using the Prandtl logarithm wind profile as

$$u_* = \frac{u_z k}{\ln\left[\frac{z}{z_o}\right]}$$
(5)

where k is the von Karman constant (0.41), u_z is the wind speed (m s^{-1}) at height z (m) above the snow surface and z_0 is the aerodynamic roughness length (m). z_0 is controlled by the saltation height and is given by

$$z_0 = \frac{c_2 c_3 u_*^2}{2g} + c_4 \lambda$$
(6)

where c_2 is the square root of the ratio of the initial vertical saltating particle velocity to u_*, c_3 is ratio of z_0 to saltation height (0.07519; Pomeroy and Gray, 1990), c_4 is a drag coefficient (0.5; Lettau, 1969) and λ is the dimensionless roughness element density.

u_{*n} is calculated using an algorithm developed by Raupach et al. (1993) for wind erosion of soil calculations that relates the partitioning of the shear stress to the geometry and density roughness elements given by

$$\frac{u_{*n}}{u_*} = \frac{(m\beta\lambda)^{0.5}}{(1+m\beta\lambda)^{0.5}}$$
(7)

where β is the ratio of element to surface drag and λ is the dimensionless roughness element density. Raupach et al. (1993) found $\beta \approx 170$ which is used for shortgrass and crop stalks. m is an empirical coefficient to account for the difference in average and maximum surface shear stress to initiate erosion. The default value for m in PBSM is 1.0 for grass and cereal grain stalks. Wyatt and Nickling (1997) determined a mean $\beta = 202$ and mean $m = 0.16$ for desert creosote shrubs (*Larrea tridentata*) in a Nevada desert. Wyatt and Nickling's β and m are presumed to be more suitable for shrubs

found in northern and western Canada than the grass and cereal grain default values in PBSM. λ is calculated as per Pomeroy and Li's (2000) modification of an original equation by Lettau (1969)

$$\lambda = N d_v \left(h_v - \frac{S}{\rho_s} \right) \tag{8}$$

5 where N is the vegetation number density (number m^{-2}), d_v is the vegetation stalk diameter (m), h_v is the height of vegetation and the snow depth is snow accumulation, S, divided by snow density ($kg\,m^{-3}$).

$u*_t$ is calculated from the meteorological history of the snowpack using an algorithm developed by Li and Pomeroy (1997a) from observations at low vegetation sites in the
10 Canadian prairies.

F_{susp} is calculated as a vertical integration from a reference height near the top of the saltation layer, $h*$, to the top of the blowing snow boundary layer (z_b), given by Pomeroy and Male (1992)

$$F_{susp} = \frac{u*}{k} \int_{h*}^{z_b} \eta(z) \ln\left(\frac{z}{z_0} \right) dz \tag{9}$$

15 where k is von Kármán's constant (0.41), η is the mass concentration of blowing snow at height z (m) and z_0 is the aerodynamic roughness height. z_b is governed by the time available for the vertical diffusion of snow particles from $h*$, calculated using turbulent diffusion theory and the logarithmic wind profile. $h*$ increases with friction velocity and is estimated as given by Pomeroy and Male (1992)

20 $$h* = 0.08436 u*^{1.27} \tag{10}$$

For fully-developed flow it is constrained at $z_b = 5$ m. At z_b shear stress is constant ($d\tau/dt=0$) and suspension occurs under steady-state conditions ($d\eta/dt=0$). Note that

Hydrological response unit-based blowing snow modelling

M. K. MacDonald et al.

as suspension diffuses from the saltation layer, saltation must be active for suspension to proceed.

E_B is calculated as a vertical integration of the sublimation rate of a single ice particle with the mean particle mass being described by a two-parameter gamma distribution of particle size that varies with height. The vertically integrated sublimation rate is given by

$$E_B = \int_0^{z_b} \frac{1}{m(z)} \frac{dm}{dt}(z)\eta(z)\,dz \tag{11}$$

where m is the mean mass of a single ice particle at height z. The rate that water vapour can be removed from the ice particle's surface layer, dm/dt, is calculated assuming particles to be in thermodynamic equilibrium. dm/dt is controlled by radiative energy exchange convective heat transfer to the particle, turbulent transfer of water vapour from the particle to the atmosphere and latent heat associated by sublimation, and is given by Schmidt (1972). E_B calculations are highly sensitive to ambient relative humidity, temperature and wind speed (Pomeroy et al., 1993; Pomeroy and Li, 2000).

Field observations show that blowing snow is a phenomenon that is unsteady over both space and time. The time steps most frequently used in PBM studies (i.e. 15, 30 or 60 min) do not match the highly variable and intermittent nature of blowing snow. In addition, small scale spatial variability in snowcover properties produce sub-element (e.g. grid cell or HRU) variability in snow transport. Li and Pomeroy (1997b) developed an algorithm to upscale blowing snow fluxes from point to area. The probability of blowing snow occurrence, p, is approximated by a cumulative normal distribution as a function of mean wind speed (location parameter), the standard deviation of wind speed (scale parameter). Empirical equations for the location and scale parameter were developed from six years of data collected at 15 locations in the Canadian prairies and are calculated from the number of hours since the last snowfall and the ambient atmospheric temperature.

3.3 Energy-Budget Snowmelt Model

EBSM (Gray and Landine, 1988) calculates the amount of snowmelt using the energy equation and is appropriate for cold weather and shallow snow simulations. The amount of snowmelt is calculated using

$$M = \frac{Q_m}{\rho h_f B} \tag{12}$$

where Q_m is the energy available for melt, ρ is the density of water, h_f is the latent heat of fusion (333.5 kJ kg^{-1}) and B is the thermal quality of snow or the fraction of ice in a unit mass of wet snow (0.95–0.97). Q_m is calculated from the energy equation as

$$Q_m = Q_n + Q_h + Q_e + Q_g + Q_p + Q_A + \Delta U / \Delta t \tag{13}$$

where Q_m is the energy available for melt, Q_n is the net radiation (incoming and outgoing shortwave and longwave radiation), Q_h is the convective sensible heat flux, Q_e is the convective latent heat flux, Q_g is the conductive ground heat flux, Q_p is the advective heat from rainfall, Q_A is the small-scale advective heat from bare ground and $\Delta U/\Delta t$ is the change in internal energy of the snow mass (all components in W m^{-2}). Equations for turbulent transfer of sensible and latent heat were derived from detailed measurements over melting snow at a prairie site.

Snow albedo, α, during winter is estimated using the method outlined by Gray and Landine (1987). The albedo depletion was approximated by three lines of different slope representing three periods: pre-melt, melt and post-melt.

The net radiation at the snow surface, Q_n, is calculated as a linear function of the daily net shortwave radiation, α and the ratio of actual to potential bright sunshine hours, n/N which is calculated in Global. Q_n is given by

$$Q_n = -0.53 + 0.47 Q_O \left(0.52 + 0.52 \left[\frac{n}{N}\right]\right)(1 - A(t)) \tag{14}$$

Title Page

Abstract | Introduction

Conclusions | References

Tables | Figures

◄ | ►

◄ | ►

Back | Close

Full Screen / Esc

Printer-friendly Version

Interactive Discussion

3.4 Needleleaf

The CRHM Needleleaf module calculates shortwave and longwave radiation exchange at the snow surface beneath a needleleaf forest canopy. Shortwave transmissivity through the forest canopy is given by a Beer-Bouger type formulation given by

$$\tau_C = \exp(-k\ell) \tag{15}$$

where k is the shortwave irradiance extinction coefficient and ℓ transmission path-length. Needleleaf does not explicitly account for radiation scattering within the canopy and the various transmissivities of different spectra, and does not have separate calculations for canopy foliage, trunks and gaps. These model omissions are accounted for by effective values for LAI.

3.5 Trees

The CRHM Trees module calculates input to the ground surface water mass beneath a forest canopy by estimating the canopy throughfall of rain and snow, the canopy interception and evaporation of rain, the canopy interception and sublimation of snow, the unloading of intercepted snow and the drip of intercepted rain.

Canopy interception of rain is calculated using a sparse Rutter interception model (Valente, 1997) where only canopy rain storage is accounted for. The fraction of rainfall intercepted by the canopy is determined from the horizontal canopy coverage which is estimated from the effective leaf area index (LAI') using an expression developed by Pomeroy et al. (2002). Evaporation of intercepted rainfall is calculated using the Penman-Monteith combination formulae (Monteith, 1965) for which the evaporation from a "fully-wetted" canopy is equal to the potential evaporation.

Canopy interception of snowfall and sublimation of intercepted snow is calculating using relationships presented by Pomeroy et al. (1998). The amount of intercepted snow is calculated as

$$I_S = I_S^* \left(1 - e^{-C_1 P_S / I_S^*}\right) \tag{16}$$

where C_1 is the dimensionless canopy-leaf contact per ground, P_S is snowfall and I_s^* is the maximum intercepted snowload which is estimated as a function of the maximum snowload per unit area of branch, the density of falling snow and LAI'. The sublimation of intercepted snow is calculated by adjusting the sublimation rate of an ice sphere by
5 an intercepted snow exposure coefficient (Pomeroy and Schmidt, 1993).

3.6 Ryan/MicroMet windflow model

The Ryan/MicroMet distributed windflow algorithm (hereafter RMM) is part of the MicroMet meteorological model (Liston and Sturm, 2006). A wind direction diverting parameterization developed by Ryan (1977) is critical to its distributed application. RMM
10 takes a reference wind speed and direction and calculates distributed wind speed direction over a DEM. RMM does not account for vegetation cover effects on windflow.
  Wind speed and direction are converted to zonal and meridional components to avoid problems with interpolating over 0°/360°. From a DEM, RMM calculates topographic slope, azimuth and curvature at each grid cell. Grid cell curvature, Ω_C, is
15 calculated from the elevation of opposing grid cells in four directions and the average of these four curvature values is the curvature of the grid cell of interest. Ω_C is given by

$$\Omega_C = \frac{1}{4}\left[\frac{z - 1/2(z_W + z_E)}{2\eta} + \frac{z - 1/2(z_S + z_N)}{2\eta} + \frac{z - 1/2(z_{SW} + z_{NE})}{2\sqrt{2}\eta} + \frac{z - 1/2(z_{NW} + z_{SE})}{2\sqrt{2}\eta}\right] \quad (17)$$

where z_N, z_{SW}, etc. are the elevation of cells in directions north, southwest, etc. of
20 the cell of interest at the curvature length scale η (m) from the cell of interest. The curvature length scale is approximately equal to a half wavelength of a topographic feature with the DEM (e.g. distance from a ridge to a valley bottom).
  The slope in the direction of the wind, Ω_S, is given by

$$\Omega_S = \beta \cos(\theta - \xi) \quad (18)$$

25 where β is the terrain slope, θ is the wind direction and ξ is the terrain slope azimuth.

The modified wind speed at the cell of interest is given by

$$W_T = W_W W \tag{19}$$

where W is the reference wind speed and W_W is the wind weight calculated using

$$W_W = 1 + \gamma_S \Omega_S + \gamma_C \Omega_C \tag{20}$$

where γ_s and γ_c are the weights assigned to the slope and curvature functions, respectively.

In this study, the η, γ_s and γ_c parameters were calibrated using the Dynamically Dimensioned Search algorithm (DDS; Tolson and Shoemaker, 2007). DDS is an automatic heuristic stochastic single-solution based global search algorithm presented by Tolson and Shoemaker (2007). The algorithm was designed to find "good" global solutions, as opposed to globally optimal solutions, within a specified number of model evaluations. The algorithm is scaled such that it initially searches globally and searches more locally as the number of iterations approaches the specified number of model evaluations. The transition from global to more local search occurs as the number of parameters being calibrated at each iteration is reduced. The parameters perturbed at each iteration are randomly selected at a magnitude randomly sampled from a normal distribution of parameter values.

4   Fisera ridge parameterization

HRUs were selected by grouping snow depths measured along the FR transect (Fig. 4). These manual snow depth measurements capture the spatial variability in aerodynamic characteristics along the FR transect which is the landscape attribute that exerts the strongest control on winter snow accumulation. As well, solar radiation and vegetation cover vary along the FR transect.

Five HRUs were selected based on the observed snow depths shown in Fig. 4. The north-facing slope HRU (NF) is located from 127 to 243 m, the ridge-top HRU (RT) is

Title Page

Abstract | Introduction

Conclusions | References

Tables | Figures

◄ | ►

◄ | ►

Back | Close

Full Screen / Esc

Printer-friendly Version

Interactive Discussion

located from 90 to 127 m, the upper south-facing slope (SF-upper) is located from 28 to 90 m, the lower south-facing slope (SF-lower) is located from 0 to 28 m and the Forest HRU is located from 0 to −15 m. Note that the contributing area of the NF HRU extends downslope beyond the extent of the manual snow survey transect to the base of the
5 slope and was established using the LiDAR-derived DEM.

The HRUs follow an aerodynamic sequence in that the model always transports snow from upwind to downwind HRUs. The HRU snow transport sequence is NF → RT → SF-upper → SF-lower → Forest (i.e. NF snow transport reaches all of RT, SF-upper, SF-lower and Forest; SF-upper snow transport only reaches SF-lower and
10 Forest; etc.).

Key CRHM model parameters are presented in Table 1. Note that the Needleleaf and Trees modules were only applied to the Forest HRU. All parameters were set based on either field measurements or default/typical values with the exception of vegetation height on the NF and RT. Shorter shrub heights than measured were needed to scour
15 enough snow from these HRUs. PBSM is parameterized for densely spaced, narrow crop stalks and grass. Shorter vegetation heights parameters were required to represent sparse shrubs on the NF and RT HRUs. Average HRU aspect and slope were determined from the DEM. A blowing snow fetch distance of 300 m was specified for each HRU as this is the minimum value required for the fully-developed flow calcula-
20 tions performed by PBSM.

Simulations were performed for 2007/2008 and 2008/2009 applying the ridge-top station air temperature, relative humidity and incoming longwave radiation observations to all HRUs. Incoming shortwave radiation observations from the ridge-top station (considered a flat plane) were applied to each HRU after adjustments for aspect and
25 slope made by the Global and Slope_Qsi modules. Simulations were performed using two different sets of wind speed forcing data:

1. FR station observed wind speed data; and

2. RMM-modelled wind speeds.

For (1), the north-facing meteorological station wind speed data was applied to the NF, the ridge-top meteorological station wind speed data was applied to the RT, and the southeast-facing meteorological station wind speed was applied to the SF-upper, SF-lower and Forest.

For (2), average RMM-modelled wind speeds were applied to each of the five HRUs. Wind speed and direction observations from an alpine meteorological station were used as reference for RMM (Fig. 5). RMM was implemented in MATLAB to simulate wind speed over the 10 m LiDAR-derived DEM. A MATLAB m-file containing the DDS algorithm (available at http://www.civil.uwaterloo.ca/btolson/software.htm) was coupled to RMM to automatically calibrate the η (Eq. 17), γ_s and γ_c (Eq. 20) parameters. 26 937 non-continuous wind speed and direction measurements from 29 January to 1 May 2009 from the reference alpine station were used to automatically calibrate the parameters to measured wind speed at the three FR stations. The optimum parameter set following 1000 objective functions evaluations of the root mean squared error (RMSE) of measured wind speed yield a RMSE of 3.4 m s^{-1} and a model bias of 0.627 (Fig. 6). The optimum parameter set was η=799 m, γ_s=0.89 and γ_c=0.11. Though the RMM model performance can be considered poor, it may be adequate for modelling blowing snow over an entire season considering the slope of the regression line is near 1:1 (modelled:measured). Time series of the RMM-modelled wind speed and the observed wind speed at the ridge-top station suggest some potential for this application (Fig. 7).

For (2), the wind speed forcing for each HRU was obtained by multiplying the reference alpine wind speed measurements by the average RMM W_W over each HRU in Eq. (20). Average RMM W_W for each HRU are presented in Table 1. The RMM W_W values along the FR transect (Fig. 8) do show some corroboration with the observed snow depth (Fig. 4).

5 Model evaluation

Simulated snow accumulation was evaluated using model bias and root mean squared error, given by

$$MB = \frac{\sum \alpha SWE_{sim}}{\sum \alpha SWE_{obs}} - 1 \tag{21}$$

$$RMSE = \sqrt{\frac{\sum (\alpha SWE_{sim} - \alpha SWE_{obs})^2}{n}} \tag{22}$$

where SWE_{sim} and SWE_{obs} are the simulated and observed SWE, respectively. α is the fractional area of the HRU. α is included so that the model evaluation statistics reflect the relative size of different HRUs that make up the FR transect. n is the number of observation-simulation pairs used to evaluate RMSE. Positive and negative MB indicate the percent by which SWE is either overestimated or underestimated throughout the simulation, respectively. The RMSE gives a measure of the variation of residuals between observed and simulated SWE in mm SWE.

6 Results

Simulations were performed at 15-min intervals from 20 October 2007 to 30 April 2008 and from 24 September 2008 to 19 April 2009. Figures 9 and 10 show observed and simulated snow accumulation over HRUs using observed station wind speed data and using RMM-modelled wind speeds, respectively. Tables 2 and 3 show end-of-winter snow accumulation, cumulative snowmelt, transport in to and out of HRUs and blowing snow sublimation, for simulations using observed wind speed data and using RMM-modelled wind speeds, respectively.

7 Discussion

Table 4 shows model evaluation statistics for all simulations over the entire simulation period. Snow accumulation was generally well simulated when using the observed wind speed data. 2008/2009 was not simulated to the same accuracy as 2007/2008 as snow accumulation was overestimated on the RT, and on the other downwind HRUs throughout the simulation until the final manual snow measurement date on 19 April 2009. Snow accumulation on the NF and RT were reduced to roughly one-third of cumulative snowfall whereas snow accumulation on the SF-lower and Forest was nearly doubled compared to cumulative snowfall due to snow redistribution by wind. Snowmelt was considerably greater during 2008/2009 than during 2007/2008. It must be noted that 56% of melt occurred by mid-October 2008, whereas the 2007/2008 simulations did not begin until mid-October 2007. Nonetheless there was considerably more winter snowmelt during 2008/2009 than during 2007/2008.

Snow accumulation was not as well simulated when using the RMM wind speeds. RMM wind speeds were typically greater than the measured wind speeds. This caused much greater erosion of the SF-upper as well as greater erosion of the RT. This increased snow transport balanced the higher blowing snow sublimation rates to yield satisfactory snow accumulation on the SF-lower and Forest through the winter. Higher snowmelt was simulated when using the RMM wind speeds (particularly for 2007/2008) because the higher RMM wind speeds increased turbulent transfer of sensible and latent heat. As well, greater melt rates were calculated for shallower snowpacks (caused by greater snow erosion rates by higher RMM wind speeds).

Two major issues are evident in the snow accumulation simulations using RMM wind speeds when examining results beyond the entire-winter snow accumulation results presented in Table 4. First, there was an approximate 17% discrepancy between estimated blowing snow sublimation quantities when using the measured and modelled wind speeds. Second, end-of-winter snow accumulation was considerably underestimated when using the RMM wind speeds (Table 5). This was caused by

Title Page

Abstract | Introduction

Conclusions | References

Tables | Figures

|◄ | ►|

◄ | ►

Back | Close

Full Screen / Esc

Printer-friendly Version

Interactive Discussion

excessive snowpack erosion on upwind HRUs, greater blowing snow sublimation rates and greater snowmelt rates caused by the higher wind speed forcing. This error will likely cause substantial difficulties in accurately simulating snowcover ablation and runoff during melt-dominated periods from May–June.

Estimated blowing snow sublimation losses ranged from 23% (low MB for 2007/2008 simulation using observed wind speed data) to 41% (low MB for 2008/2009 simulation using RMM wind speeds) over the transect. These blowing snow sublimation losses were substantial and important to the winter water balance of the alpine ridge. Satisfactory FR snow mass balance closure suggests that the use of the minimum PBSM fetch distance parameter (300 m) is adequate in this environment. Boundary layer development for fetches shorter than this in complex terrain are poorly understood and so the parameter is left to its minimum value (based on the limits of PBSM physics) until a more realistic parameterization can be developed.

The observed SF-lower snow accumulation was greater than the Forest snow accumulation in 2008/2009, whereas the opposite was true during 2007/2008 and for the simulations. It is difficult to elucidate why this was the case. Observed wind speeds were generally higher during 2008/2009 than 2007/2008 (higher mean and less positive skew of wind speed), so it is not a case of downwind transport distance increasing with increasing wind speed; in fact the inverse seems to have occurred.

The static definition of the HRU locations and relative lengths is a simplification of the actual spatiotemporal snow redistribution patterns. However, changing HRUs sizes during a model run would add substantial complexity to the calculation of mass balances for HRU.

It will be worthwhile testing other empirical, terrain-based windflow models (e.g. Winstral et al., 2009). It is not expected that empirical windflow models can be as accurate as the much more computational expensive computational fluid dynamic models. It is worth mentioning that Bernhardt et al. (2009) applied a computationally inexpensive approach to use wind fields generated from the MM5 atmospheric model to drive a snow transport model by generating a library of the 220 most common windfields.

8 Conclusions

Snow redistribution and the resulting accumulation regimes were simulated over HRUs representing a transect along an alpine ridge in the Canadian Rockies. This study shows that snow accumulation can be adequately simulated for HRUs over mountainous terrain using physically based blowing snow and snowmelt models. An HRU-based discretization can be a much more computationally efficient approach than fully-distributed ones. This is particularly relevant for modelling snow redistribution within large-scale hydrology models and land surface schemes. HRUs were selected by examining manual snow depth measurements. Future work will involve generalizing HRUs based on terrain characteristics.

Snow redistribution by wind significantly controls snow accumulation regimes in mountain environments. Snow transport from windward slopes and ridge-tops reduced snow accumulation in these landscapes to less than one-third of snowfall, and nearly doubled snow accumulation in parts of leeward slopes and at the treeline. Blowing snow sublimation losses are significant and were estimated to be approximately one-quarter of seasonal snowfall.

The empirical RMM model performed adequately well in simulating winter snow accumulation and redistribution, but substantially underestimated the end of winter snow accumulation that governs snowmelt runoff. The RMM model also performed poorly in estimating wind speed. The wind speed overestimation gave rise to a sublimation overestimation which resulted in an underestimation of end-of-winter snow accumulation. This would cause further difficulties in accurately simulating snowcover ablation and runoff during snowmelt.

References

5 Bernhardt, M., Zängl, G., Liston, G. E., Strasser, U., and Mauser, W.: Using wind fields from a high-resolution atmospheric model for simulating snow dynamics in mountainous terrain, Hydrol. Process., 23, 1064–1075, 2009.

Bintanja, R.: The contribution of snowdrift sublimation to the surface mass balance of Antarc-tica, Ann. Glaciol., 27, 251–259, 1998.

10 Budd, W. F., Dingle, W. R. J., and Radok, U.: The Byrd snow drift project: outline and basic results, in: Studies in Antarctic Meteorology, American Geophysical Union, Antar. Res. S., 9, 71–134, 1966.

Dornes, P. F., Pomeroy, J. W., Pietroniro, A., Carey, S. K., and Quinton, W. L.: Influence of landscape aggregation in modelling snow-cover ablation and snowmelt runoff in a sub-arctic

15 mountainous environment, Hydrolog. Sci. J., 53, 725–740, 2008.

Dyunin, A. K.: Fundamentals of the theory of snowdrifting, Isvestia Sibirski Otdeleniya Akademii Nauk SSSR, 12, 11–24, 1959 (translation: Belkov, G., National Research Council of Canada Technical Translation 952, 26 pp., 1961).

Essery, R., Li, L., and Pomeroy, J.: A distributed model of blowing snow over complex terrain,

20 Hydrol. Process., 13, 2423–2438, 1999.

Frazer, G. W., Canham, C. D., and Lertzman, K. P.: Gap Light Analyzer GLA, Version 2.0, Imaging software to extract canopy structure and gap light transmission indices from true-color fisheye photographs, Users manual and program documentation, Institute of Ecosys-tem Studies, Simon Fraser University, Burnaby, B.C., Milbrook, NY, 40 pp., 1999.

25 Gray, D. M. and Landine, P. G.: Albedo model for shallow prairie snowcovers, Can. J. Earth. Sci., 24, 1760–1768, 1987.

Gray, D. M. and Landine, P. G.: An energy-budget snowmelt model for the Canadian Prairies, Can. J. Earth. Sci., 25, 1292–1303, 1988.

Jones, H. G., Pomeroy, J. W., Walker, D. A., and Hoham, R. W.: Snow Ecology: An Interdisciplinary Examination of Snowcovered Ecosystems, Cambridge University Press, Cambridge, UK, 394 pp., 2001.

Kasten, F. and Young, A. T.: Revised optical air-mass tables and approximation formula, Appl. Optics, 28, 4735–4738, 1989.

Lettau, H.: Note on aerodynamic roughness-parameter estimation on the basis of roughness element description, J. Appl. Meteorol., 8, 828–832, 1969.

Li, L. and Pomeroy, J. W.: Estimates of threshold wind speeds for snow transport using meteorological data, J. Appl. Meteorol., 36, 205–213, 1997a.

Li, L. and Pomeroy, J. W.: Probability of occurrence of blowing snow, J. Geophys. Res., 102, 21955–21964, 1997b.

Liston, G. E. and Sturm, M.: A snow transport model for complex terrain, J. Glaciol., 44, 498–516, 1998.

Liston, G. E. and Sturm, M.: Winter precipitation patterns in arctic Alaska determined from a blowing-snow model and snow-depth observation, J. Hydrometeorol., 3, 646–659, 2002.

Liston, G. E. and Elder, K.: A meteorological distribution system for high-resolution terrestrial modeling (MicroMet), J. Hydrometeorol., 7, 217–234, 2006.

MacDonald, J. P. and Pomeroy, J. W.: Gauge undercatch of two common snowfall gauges in a prairie environment, in: Proceedings of the 64th Eastern Snow Conference, St. John's, Canada, 29 May–1 June 2007, 119–124, 2007.

MacDonald, M. K., Pomeroy, J. W., and Pietroniro, A.: Parameterizing redistribution and sublimation of blowing snow for hydrological models: tests in a mountainous subarctic catchment, Hydrol. Process., 23, 2570–2583, 2009.

Pomeroy, J. W.: A process-based model of snow drifting, Ann. Glaciol., 13, 237–240, 1989.

Pomeroy, J. W.: Transport and sublimation of snow in wind-scoured alpine terrain, in: Snow, Hydrology and Forests in Alpine Areas, edited by: Bergman, H., Lang, H., Frey, W., Issler, D., and Salm, B., IAHS Press, 205, Wallingford, UK, 131–140, 1991.

Pomeroy, J. W. and Gray, D. M.: Saltation of snow, Water Resour. Res., 26, 1583–1594, 1990.

Pomeroy, J. W and Gray, D. M.: Snowcover Accumulation, Relocation and Management, National Hydrological Research Institute Science Report, 7, Environment Canada, Saskatoon, Canada, 144 pp., 1995.

Hydrological response unit-based blowing snow modelling

M. K. MacDonald et al.

Pomeroy, J. W., Gray, D. M., Brown, T., Hedstrom, N. R., Quinton, W., Granger, R. J., and Carey, S. K.: The cold regions hydrological model: a platform for basing process representation and model structure on physical evidence, Hydrol. Process., 21, 2650–2667, 2007.

Pomeroy, J. W., Gray, D. M., Hedstrom, N. R., and Janowicz, J. R.: Prediction of seasonal snow accumulation in cold climate forests, Hydrol. Process., 16, 3543–3558, 2002.

Pomeroy, J. W., Gray, D. M., and Landine, P. G.: Modelling the transport and sublimation of blowing snow on the prairies, in: Proceedings of the 48th Eastern Snow Conference, Guelph, Canada, 5–7 June 1991, 175–188, 1991.

Pomeroy, J. W., Gray, D. M., and Landine, P. G.: The Prairie Blowing Snow Model: characteristics, validation and operation, J. Hydrol., 144, 165–192, 1993.

Pomeroy, J. W. and Li, L.: Prairie and arctic areal snow cover mass balance using a blowing snow model, J. Geophys. Res.-Atm., 105, 26619–26634, 2000.

Pomeroy, J. W. and Male, D. H.: Steady-state suspension of snow, J. Hydrol., 136, 275–301, 1992.

Pomeroy, J. W., Marsh, P., and Gray, D. M.: Application of a distributed blowing snow model to the Arctic, Hydrol. Process., 11, 1451–1464, 1997.

Pomeroy, J. W., Parviainen, J., Hedstrom, N., and Gray, D. M.: Coupled modelling of forest snow interception and sublimation, Hydrol. Process., 12, 2317–2337, 1998.

Pomeroy, J. W. and Schmidt, R. A.: The use of fractal geometry in modelling intercepted accumulation and sublimation, in: Proceedings of the 50th Eastern Snow Conference, Quebec City, Canada , 8–10 June 1993, 1–10, 1993.

Raupach, M. R., Gillette, D. A., and Leys, J. F.: The effect of roughness elements on wind erosion threshold, J. Geophys. Res., 98, 3023–3029, 1993.

Ryan, B. C.: A mathematical model for diagnosis and prediction of surface winds in mountainous terrain, J. Appl. Meteorol., 16, 571–584, 1977.

Schmidt, R. A.: Sublimation of wind-transported snow – a model, United States Department of Agriculture, Forest Service, Rocky Mountain Forest and Range Research Station, Fort Collins, United States of America, RM-90, 24 pp., 1972.

Schmidt, R. A.: Transport rate of drifting snow and the mean wind speed profile, Bound.-Lay. Meteorol., 34, 213–241, 1986.

Stevenson, D. R.: Geological and groundwater investigations in the Marmot Creek experimental basin of southwestern Alberta, Canada, M.Sc. thesis, University of Alberta, Edmonton, Canada, 1967.

Hydrological response unit-based blowing snow modelling

M. K. MacDonald et al.

Title Page

Abstract | Introduction

Conclusions | References

Tables | Figures

|◄ | ►|

◄ | ►

Back | Close

Full Screen / Esc

Printer-friendly Version

Interactive Discussion

Takeuchi, M.: Vertical profile and horizontal increase of drift-snow transport, J. Glaciology, 26, 481–492, 1980.

Tolson, B. A. and Shoemaker, C. A.: Dynamically dimensioned search algorithm for computationally efficient watershed model calibration, Water Resour. Res., 43, W01413, doi:10.1029/2005WR004723, 2007.

Valente, F., David, J. S., and Gash, J. H. C.: Modelling interception loss for two sparse eucalypt and pine forests in central Portugal using reformulated Rutter and Gash analytical models, J. Hydrol., 190, 141–162, 1997.

Utnes, T. and Eidsvik, K. J.: Turbulent flows over mountainous terrain modelled by the Reynolds equations, Bound.-Lay. Meteorol., 79, 393–416, 1996.

Winstral, A., Marks, D., and Gurney, R.: An efficient method for distributing wind speeds over heterogeneous terrain, Hydrol. Process., 23, 2526–2535, 2009.

Wyatt, V. E. and Nickling, W. G.: Drag and shear stress partitioning in sparse desert creosote communities, Can. J. Earth. Sci., 34, 1486–1498, 1997.

Hydrological response unit-based blowing snow modelling

M. K. MacDonald et al.

Title Page

Abstract	Introduction
Conclusions	References
Tables	Figures

|◄ ►|

◄ ►

Back Close

Full Screen / Esc

Printer-friendly Version

Interactive Discussion

Table 1. CRHM model parameters.

	NF	RT	SF-upper	SF-lower	Forest
Length (m)	116	37	62	28	15
Aspect (° from north)	345	30	101	93	94
Slope (°)	26	18	20	18	16
Vegetation height (m)	0.14	0.17	0.82	0.92	2.3
Vegetation density (shrubs m^{-2})	0.1	0.1	0.6	0.6	0.5
Maximum canopy snow load (kg m^{-2})	–	–	–	–	3
Maximum canopy rain load (kg m^{-2})	–	–	–	–	2
Leaf Area Index ()	–	–	–	–	0.91
RMM Wind Weight (simulated/reference)	1.49	1.16	0.93	0.92	0.98

Table 2. Summary of cumulative model results using observed wind speed data for **(a)** 2007/2008 and **(b)** 2008/2009 (quantities are in $\mathrm{kg\,m^{-2}}$; brackets indicate quantity as percentage of snowfall).

(a)

	Snow on ground		Snowmelt		Transport In		Transport Out		Sublimation	
NF	104	(28)	4.7	(1)	0	(0)	115	(31)	149	(40)
RT	133	(36)	4.4	(1)	25	(7)	120	(32)	139	(35)
SF-upper	420	(113)	4.5	(1)	54	(15)	1	(0)	1	(0)
SF-lower	612	(164)	4.6	(1)	244	(65)	0	(0)	0	(0)
Forest	741	(199)	4.5	(1)	373	(100)	0	(0)	0	(0)
Transect	276	(74)	4.6	(1)	–	–	–	–	87	(23)

(b)

	Snow on ground		Snowmelt		Transport In		Transport Out		Sublimation	
NF	25	(8)	30	(10)	0	(0)	112	(36)	159	(51)
RT	203	(66)	25	(8)	19	(6)	47	(15)	54	(18)
SF-upper	312	(100)	36	(11)	54	(17)	8	(3)	11	(4)
SF-lower	484	(152)	33	(10)	199	(63)	0	(0)	0	(0)
Forest	602	(185)	54	(17)	330	(101)	0	(0)	0	(0)
Transect	203	(65)	32	(10)	–	–	–	–	82	(26)

Table 3. Summary of cumulative model results using RMM-modelled wind speeds for **(a)** 2007/2008 and **(b)** 2008/2009 (quantities are in $kg\,m^{-2}$; brackets indicate quantity as percentage of snowfall).

(a)

	Snow on ground		Snowmelt		Transport In		Transport Out		Sublimation	
NF	17	(4)	25	(7)	0	(0)	123	(33)	208	(56)
RT	41	(11)	28	(8)	149	(40)	181	(49)	270	(68)
SF-upper	297	(80)	11	(3)	78	(21)	58	(16)	83	(21)
SF-lower	618	(166)	11	(3)	257	(69)	0	(0)	0	(0)
Forest	692	(186)	18	(5)	337	(90)	0	(0)	0	(0)
Transect	192	(52)	20	(5)	–	–	–	–	152	(41)

(b)

	Snow on ground		Snowmelt		Transport In		Transport Out		Sublimation	
NF	3	(1)	24	(8)	0	(0)	117	(38)	181	(58)
RT	17	(5)	51	(16)	122	(39)	160	(52)	205	(66)
SF-upper	236	(75)	45	(15)	100	(32)	53	(17)	79	(25)
SF-lower	490	(154)	45	(14)	217	(68)	0	(0)	0	(0)
Forest	554	(170)	75	(23)	303	(93)	0	(0)	0	(0)
Transect	146	(47)	38	(12)	–	–	–	–	130	(41)

M. K. MacDonald et al.

Table 4. Model evaluation statistics for entire simulation period.

Year	Observed Wind		RMM-modelled Wind	
	RMSE	MB	RMSE	MB
2007/2008	8.6	0.03	13.9	−0.24
2008/2009	11.5	0.19	12.5	−0.09

Table 5. Model evaluation statistics only for final pre-melt measurement date.

Date	Observed Wind		RMM-modelled Wind	
	RMSE	MB	RMSE	MB
29 April 2008	6.0	0.02	19.6	−0.29
14 April 2009	13.3	−0.09	19.0	−0.35
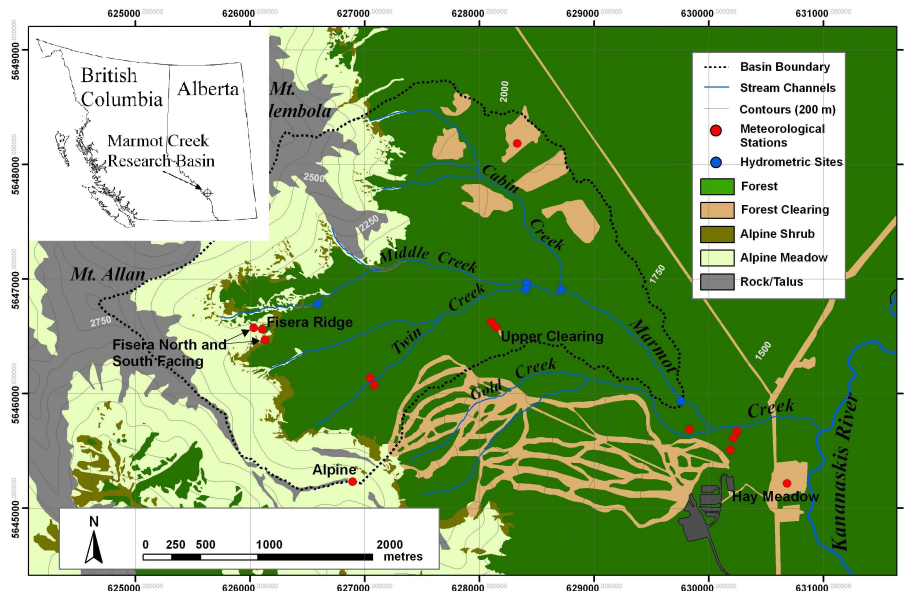
Fig. 1. Marmot Creek Basin landcover and station locations. Inset shows location of Marmot Creek Research Basin.
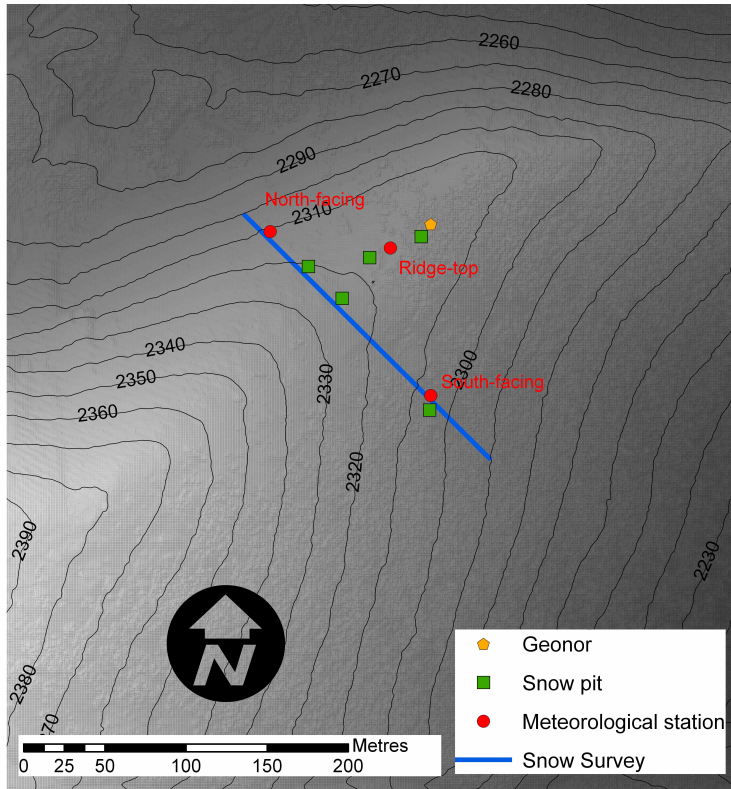
Fig. 2. Fisera Ridge meteorological station, snow survey, snow pit and Geonor locations.
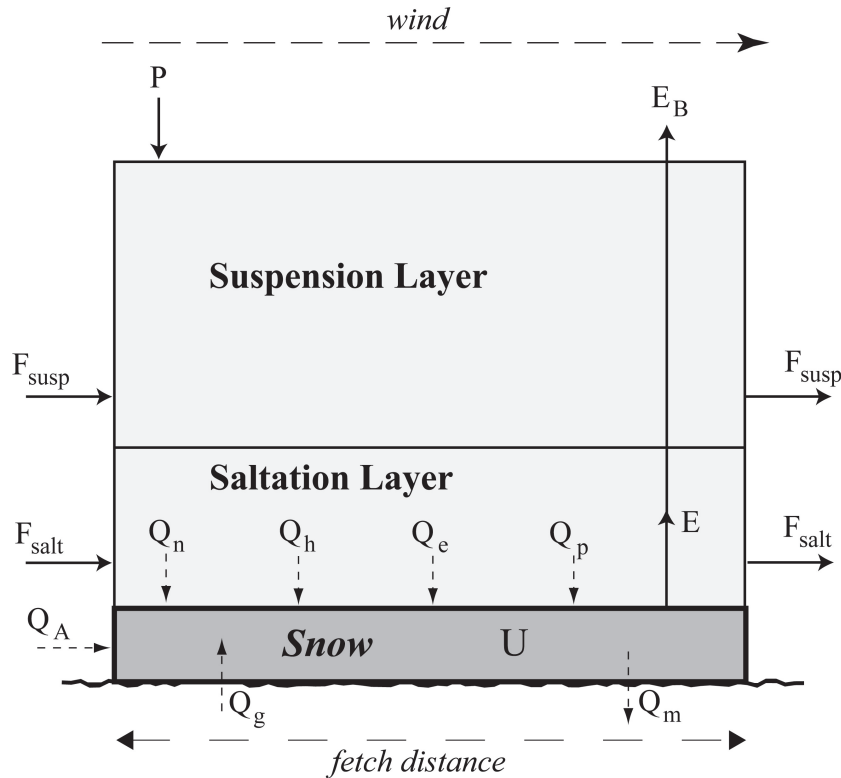
Full Screen / Esc

Fig. 3. Control volume for blowing snow mass fluxes and snowmelt energy.
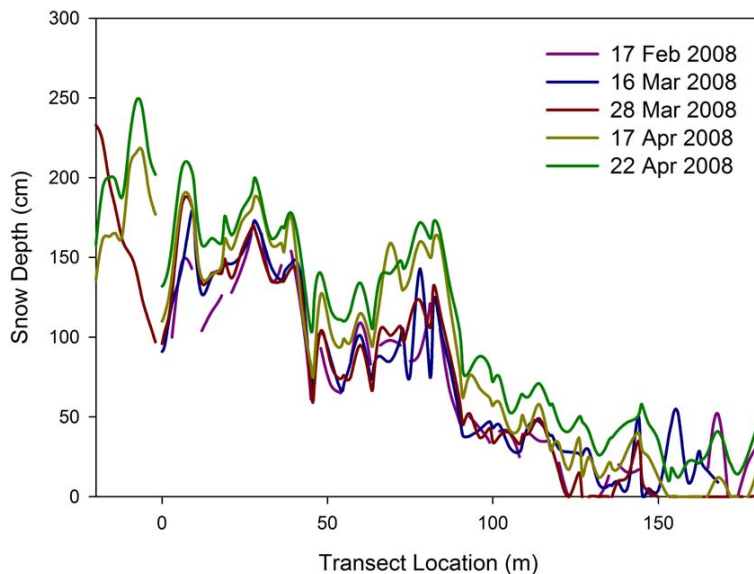
Fig. 4. Snow depth along Fisera Ridge Transect. Locations <0 m are in the forest, locations <114 m have south-facing aspect and locations >114 m have north-facing aspect.
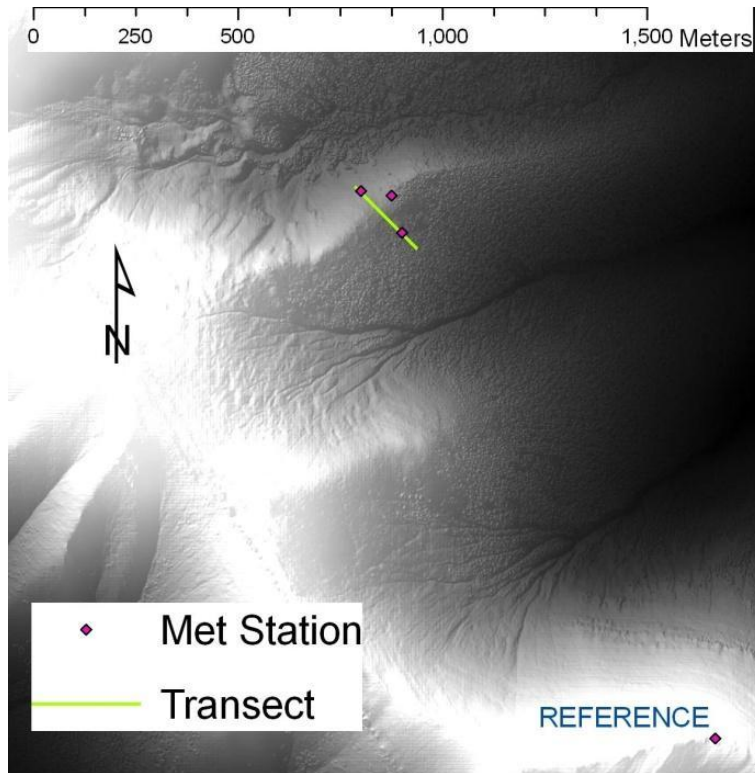
Fig. 5. Reference alpine meteorological station location relative to Fisera Ridge.

Title Page

Abstract Introduction

Conclusions References

Tables Figures

Back Close

Full Screen / Esc

Printer-friendly Version

Interactive Discussion
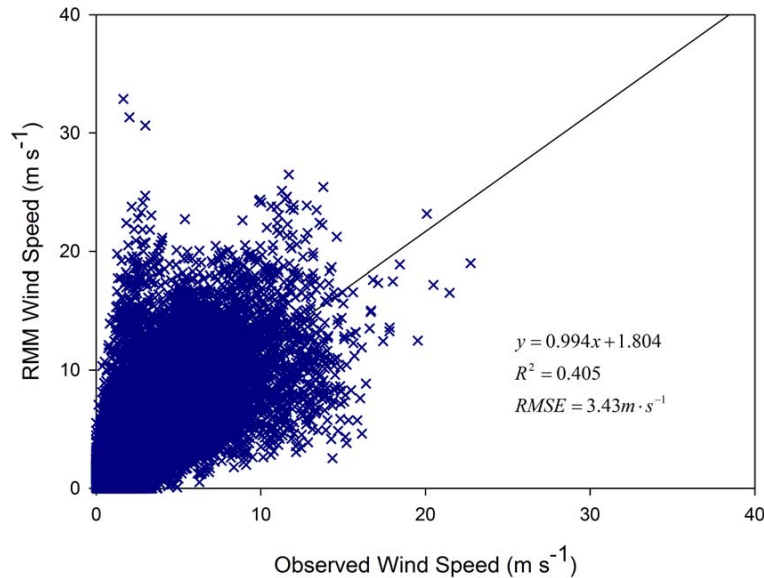
Fig. 6. Fisera Ridge observed wind speed versus RMM modelled wind speed (Solid line is a linear regression).
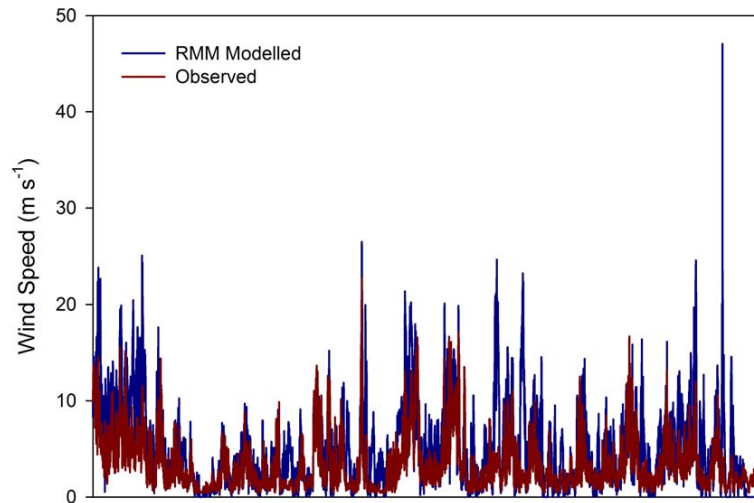
Fig. 7. Non-continuous time series of ridge-top station observed and RMM modelled wind speed.
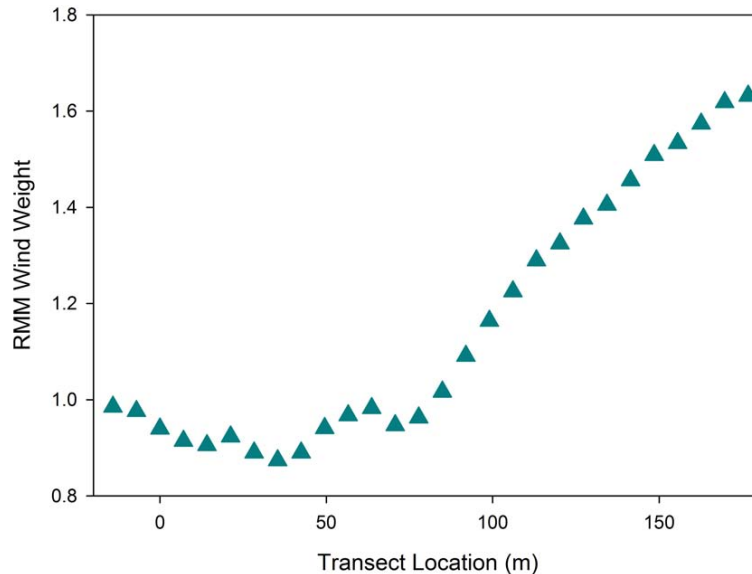
Fig. 8. RMM wind weights along Fisera Ridge Transect. Locations <0 m are in the forest, locations <114 m have south-facing aspect and locations >114 m have north-facing aspect.
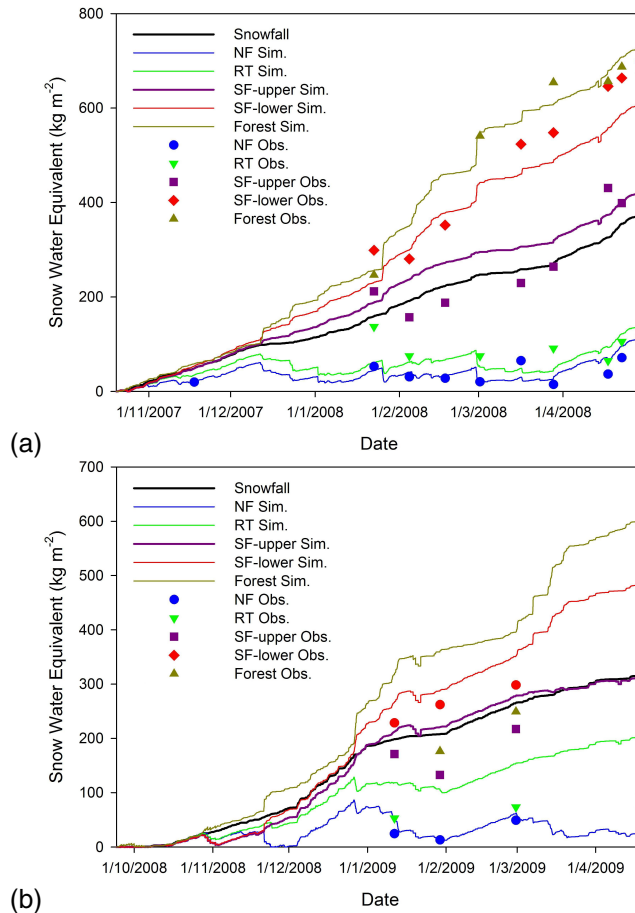
Fig. 9. Observed and simulated snow accumulation using observed wind speeds for **(a)** 2007/2008 and **(b)** 2008/2009.
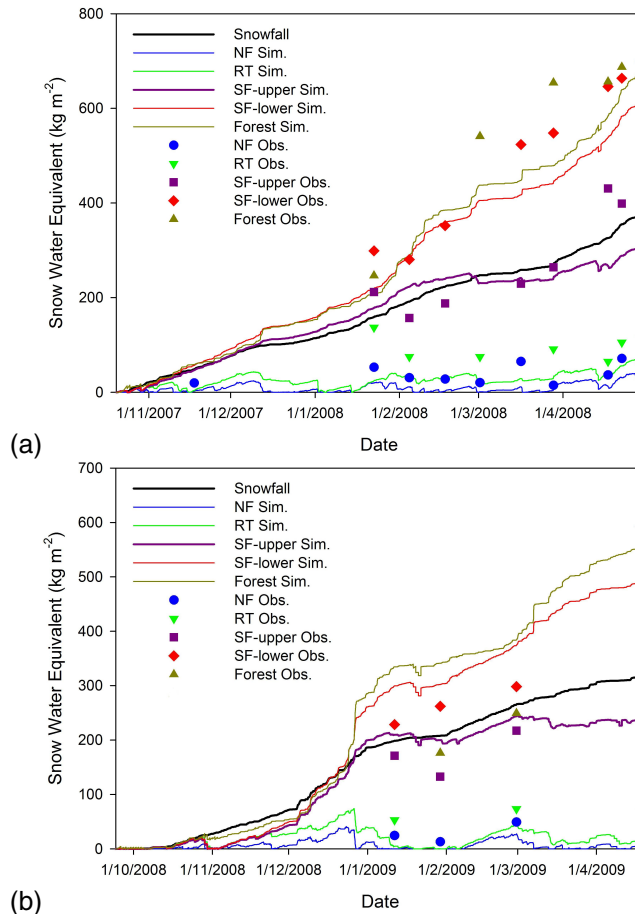
Fig. 10. Observed and simulated snow accumulation using RMM-modelled wind speeds for **(a)** 2007/2008 and **(b)** 2008/2009.

Title Page

Abstract | Introduction

Conclusions | References

Tables | Figures

◀◀ | ▶▶

◀ | ▶

Back | Close

Full Screen / Esc

Printer-friendly Version

Interactive Discussion